



Ivan Nazarenko,  
Oleg Dedov,  
Yevhen Mishchuk,  
Iryna Berynk,  
Artur Onyshchenko,  
Mykola Kuzminets,  
Valentyn Chernysh,  
Mykola Nesterenko

# DETERMINATION OF FORCE AND ENERGY PARAMETERS IN IMPACT FRACTURE PROCESSES OF MATERIALS OF VARIOUS STRENGTHS AND RHEOLOGY PROPERTIES

*The object of research is the processes of impact fracture of materials of different strengths and rheological properties.*

*The problem of determining the force and energy parameters remains the lack of a generally accepted model of the processes of fracture of materials of different strengths and their rheological properties. In most crushing machines in the crushing chamber, the destruction of materials is accompanied by impact loads or is generally shock (impact crushers).*

*The work includes studies of material destruction using the example of granite. The analysis of Johnson-Holmquist models was carried out, according to the plastic fracture model, which is designed to model the behavior of brittle materials, according to the fracture model of porous materials, especially concretes, which are subjected to large deformations, high strain rates and high pressure. It was found that during impact loading, maximum stresses arise on the impact surface, and also spread along the beam to the inner edges of the supports. The difference between the internal and kinetic energies for the JH2 body was 9.2 J, while for the JH1 body it was 15.3 J. The study on the pendulum impactor allowed to estimate the energy spent on the fracture of the material sample. It was established that if the crack crosses the intergranular boundary due to the action of local stress concentration, new cracks appear in the corresponding cleavage planes of neighboring grains, which require additional energy input to the sample. To estimate the dissipated energy in the fracture process, it was proposed to introduce an appropriate resistance coefficient. Based on experimental data, the resistance coefficient value was established for various rocks. The obtained research results can be used in the development and study of equipment for crushing materials. The value of the specific fracture energy can be used to study dynamic processes in building structures under excessive loads.*

**Keywords:** impact fracture modeling, pendulum impactor, Johnson-Holmquist rheological model, sliding contact energy, impact strength, energy dissipation factor.

Received: 03.02.2026

Received in revised form: 22.03.2026

Accepted: 03.04.2026

Published: 30.04.2026

© The Author(s) 2026

This is an open access article

under the Creative Commons CC BY license

<https://creativecommons.org/licenses/by/4.0/>

## How to cite

Nazarenko, I., Dedov, O., Mishchuk, Y., Berynk, I., Onyshchenko, A., Kuzminets, M., Chernysh, V., Nesterenko, M. (2026). Determination of force and energy parameters in impact fracture processes of materials of various strengths and rheology properties. *Technology Audit and Production Reserves*, 2 (1 (88)), 6–16. <https://doi.org/10.15587/2706-5448.2026.356852>

## 1. Introduction

The processes of material destruction are widely used in various industries, in particular in construction. One of the most common examples is the grinding of materials for the preparation of aggregates for concrete mixtures, which determines the quality and durability of structures. At the same time, understanding the patterns of material destruction is a necessary condition for the correct determination of stresses and deformations that arise in structures under the influence of dynamic loads. During the operation of technical facilities for various purposes, there is a need to take into account not only the normative loads acting on structural elements, but also the loads that may arise in the event of unforeseen events [1, 2]. Most of the research conducted in the world concerns the protection of buildings from seismic loads, however, military operations in Ukraine show the need to find solutions to protect buildings and their elements (equipment, machinery and equipment) from the dynamic destructive effects of ammunition. A comprehensive approach to modeling complex dynamic systems can

be adapted to building structures to analyze their stability, vibration sensitivity, and behavior under conditions of unpredictable factors [3]. However, the lack of generally accepted physical models that take into account rheological properties in the processes of material destruction makes it difficult to determine the real values of stresses and strains in modeling and assessing the technical condition. Classical energy laws (Rittinger, Kirpichov-Kik, Bond, Rebinder) are widely used to describe the processes of crushing and destruction, but their use has a number of limitations associated with the heterogeneity of materials and the complexity of real dynamic processes. In [4] it is shown that none of the traditional approaches provides a universal result, which necessitates the search for new methods for estimating energy parameters. Similar conclusions are confirmed in other sources that analyze energy dissipation in the processes of destruction and earthquakes [5]. The problem of multi-cracked rock failures is widespread in such fields as mining, civil engineering, petroleum engineering and geohazard assessment. Significant progress has been achieved in theory, experiments, modeling and engineering applications. Thus, the study [6] is devoted

to the processes of crack propagation under dynamic loading. The created crack propagation model is suitable only for brittle materials, but the results apply to polymeric materials, which have properties different from rocks. Significant development has been made in numerous modeling methods, in particular finite element analysis, which allows determining the stress-strain state of structures and materials under dynamic loading.

In the study [7], numerical modeling of the fracture of brittle materials using the FE-FEM method was considered, namely, modeling of rapid crack motion without mesh mixing. That is, the results do not reflect the real process of material fracture. The destruction of rocks and the prospects of numerical modeling were considered by the authors in the work [8]. The destruction processes were considered in the modeling of blasting operations during the development of rock materials in the form of a continuous mass of large mass. The process of mixing technological media also depends on the process of crushing rock. As shown in the study [9], it is the quality of crushing that determines the efficiency of mixing, which confirms the need for a comprehensive analysis of the force and energy parameters of the fracture processes. In the work [10], an analysis of methods for determining the dynamic fracture viscosity is presented. The results of the study confirm the hypothesis of the need to develop new methods to take into account the dynamic fracture viscosity. An important addition to numerical studies are experimental methods that provide verification of the adequacy of models and allow obtaining real data on the fracture processes. In works [11, 12], measurements of amplitudes and frequencies of oscillations were carried out, which confirmed the presence of wave processes and allowed to determine critical loading modes. Experimental studies of dynamic rock failure were performed in [13]. The studies were performed using the quasi-static triaxial loading method, after which shock loads (SHPB) were applied to it. The disadvantage of the work is that this model is more suitable for describing rocks at their location and does not take into account the parameters of the dynamic action of technological equipment. In work [14], a study of dynamic sandstone failure is presented. The disadvantages include the use of high-speed tensile loading and failure to take into account machine parameters. In the source [15], studies of the process of rock failure during blasting operations are given. The disadvantage of the work is the consideration of high-speed loading on rock masses, failure to take into account machine parameters. In [16], numerical modeling of dynamic rock failure was considered, using the method of discrete deformation analysis and based on Voronny tessellation. The disadvantage of this work is the lack of experimental data, the load was modeled in the form of applying a high-speed impact. Research [17] is devoted to modeling the behavior of metals under impact loading and determining the dynamic fracture toughness, the authors note the consistency of the modeling and experimental results. The convergence of the results for plastic materials suggests that this approach can be applied to brittle building materials. Similar experimental studies [18] were performed for rocks, the results are useful for understanding dynamic effects, but require more experiments on different samples and materials.

The absence of values of force and energy parameters in the processes of material failure makes it impossible to make a reasonable choice of machines and equipment for both technological processes and for the restoration of destroyed objects.

The relevance of research is due to the fact that the destruction processes have a complex force and energy nature, which depends on the strength and rheological properties of materials. Therefore, there is a need for a comprehensive approach that combines a review and analysis of existing methods for determining force and energy parameters in the destruction processes of materials, numerical modeling and experimental studies.

*The object of research* is the processes of impact destruction of materials of different strength and rheological properties.

*The aim of research* is to determine the force and energy parameters in the destruction processes of materials of different strength and their rheological properties.

To achieve the aim, the following objectives were formulated and solved:

- numerical modeling of the process of dynamic destruction of prismatic specimens with different rheological properties;
- perform experimental studies of dynamic destruction of specimens with different physic-mechanical properties;
- based on experimental data, determine the value of the resistance coefficient for different rocks.

## 2. Materials and Methods

The modeling of the impact failure process was performed in the Ansys Ls-Dyna environment. A model of a rectangular beam supported by two supports and a prismatic impactor located at a certain distance from the beam was created. Granite was used as the material for the beam, and steel for the supports and impactor. The research was performed in time (Time History) with modeling of the contact between the impactor and the material.

The impactor model is considered as a rigid body and is described by the Hooke elastic model.

To describe the model of the studied material, two models Mat\_Johnson\_Holmquist\_Ceramics and Mat\_Johnson\_Holmquist\_Concrete were used, which allow obtaining results under dynamic loading. The corresponding models best reflect the physics of fracture of brittle materials under complex loading. Models such as Coulomb-Mohr or Drucker-Prager do not contain an algorithm that can qualitatively describe the dynamic loading pattern. In addition, the proposed models adequately describe the processes of fracture, cracking of the material under dynamic loads, which is critical for the problems of impact interaction and crushing of rocks.

The Mat\_Johnson\_Holmquist\_Ceramics model is a plastic fracture model designed to simulate the behavior of brittle materials and reduce their strength under impact loads. Such materials include ceramics, glass, and others. The Mat\_Johnson\_Holmquist\_Concrete model is used to simulate concretes that are subject to large deformations, high deformation rates, and high pressure.

Experimental studies were performed at the Building Structures Testing Center of the Kyiv National University of Civil Engineering and Architecture. A pendulum impactor (Fig. 1, a) KM-30 (manufacturer ZIM, USSR, 1970) was used for the experiments, a distinctive feature of which is its modernization by the authors of the research. The test stand (Fig. 1, b) consists of a pendulum beam with an installed encoder, a control unit, and a personal computer.

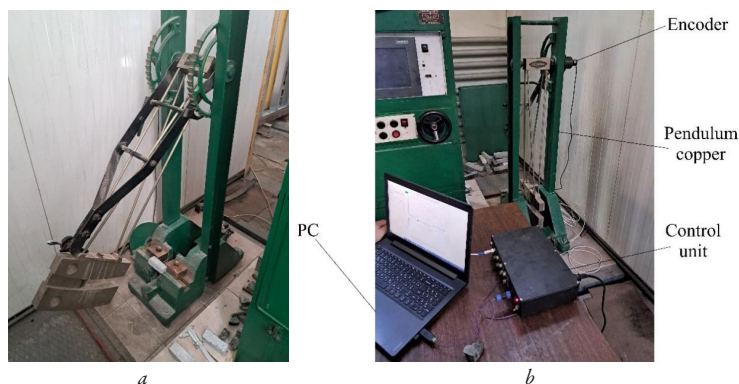


**Fig. 1.** Experimental equipment:  
a – pendulum copper; b – measuring and recording equipment

The research is based on the principle of changing the energy of the pendulum before and after the impact, the difference between which is the work done by the fracture.

In order to register the parameters of the pendulum motion, an OMRON E6B2-CWZ6C encoder (Japan) was installed on its axis of rotation. The control unit is made on the basis of the STM32F103C8T6 board (Malaysia), with a TTL UART 1 interface converter module (China) for data transmission to a PC.

Using the encoder, the angle of rotation of the pendulum axis was registered in time. With further processing of the data stream, the angle before and after the impact and the speed at the moment of impact were determined.

The following materials were selected: granite, gabbro and marble.

### 3. Results and Discussion

#### 3.1. Numerical simulation of the dynamic fracture process of prismatic specimens with different rheological properties

The Johnson-Holmquist rheological model describes the behavior of a material in two stages. In the first stage, the material is considered elastic up to a certain stress level. The second stage is beyond the yield point. When the yield point is exceeded, the material begins to accumulate damage, which reduces its strength.

The equivalent strength is defined as a function of pressure, strain rate, and damage. Pressure is defined as a function of volumetric strain and takes into account the effect of permanent fracture. Damage accumulates as a function of plastic volumetric strain, equivalent plastic strain, and pressure.

Initially, the Mat\_Johnson\_Holmquist\_Ceramics\_JH2 model was investigated.

The total stress is defined as

$$\sigma^n = \sigma_i^n - D(\sigma_i^n - \sigma_f^n), \quad (1)$$

where

$$\sigma_i^n = a(p^n + t^n)^k (1 + c \ln \dot{\epsilon}^n), \quad (2)$$

where  $a$  – the parameter of the normalized strength of the intact material;  $c$  – the strength parameter that takes into account the dependence of strength on the strain rate;  $\dot{\epsilon}^n$  – the normalized rate of plastic deformation;  $t^n = [\sigma_p] / p_{HEL}$ ,  $p^n = p / p_{HEL}$ , where  $p_{HEL}$  – the pressure component at the Hugoniot yield point,  $[\sigma_p]$  – the maximum tensile strength,  $p$  – the pressure;  $k$  – the pressure index for the integral material, determined by the variable  $n$ .

The stress in formula (2) reflects the behavior of the material before its damage (stress in the material that has not started to collapse). The index  $n$  in dependencies (1) and (2) indicates the normalized value. The stress and pressure are normalized by the equivalent stresses at the Hugoniot yield point. The strain rate is normalized by the reference strain rate determined in the initial data.

The parameter  $D$  represents the accumulation of fracture, which is based on the increase in plastic deformation per computational cycle and plastic deformation before fracture. It is determined based on the dependence

$$D = \sum \frac{\Delta \epsilon^p}{\epsilon_f^p}. \quad (3)$$

In turn, the plastic deformation before failure is defined as

$$\epsilon_f^n = d_1 (p^n + t^n)^{d_2}, \quad (4)$$

the parameter  $\sigma_f^n$  reflects the behavior of failure and is determined

$$\sigma_f^n = b(p^n)^m (1 + c \ln \dot{\epsilon}^n) \leq \sigma_{Fmax}, \quad (5)$$

where  $\sigma_{Fmax}$  – the maximum cracking strength (when set to 0.0 by the program, then  $\sigma_{Fmax} = 10^{20}$ );  $b$  – the normalized strength of the damaged material (indicates how much the material can withstand the load after its failure);  $m$  – the pressure exponent for the damaged material (determines how much pressure affects the strength of the damaged material). The parameter  $d_1$  controls the rate of damage accumulation. If the value  $d_1 = 0$  is set, then complete failure occurs instantly in one time step.

The hydrostatic pressure in an undamaged material during compression is determined by the following equation

$$p = k_1 \xi + k_2 \xi^2 + k_3 \xi^3. \quad (6)$$

Under tensile conditions, equation (6) is somewhat simplified

$$p = k_1 \xi, \quad (7)$$

where  $\xi = \rho / \rho_0 - 1$ ,  $\rho$  – the density of the material during loading;  $\rho_0$  – the initial density of the material in the unloaded state. Part of the elastic energy loss is converted into hydrostatic potential energy. This part of the energy is determined by the parameter  $\beta$  and is programmatically set in the range from 0 to 1.

The limit The Hugoniot elasticity determines the maximum stress at which a material behaves elastically under impact loads. This limit is determined by the equality

$$\sigma_{hel} = k_1 \xi_h + k_2 \xi_h^2 + k_3 \xi_h^3 + \frac{4}{3} G \left( \frac{\xi_h}{1 + \xi_h} \right), \quad (8)$$

where  $\xi_h$  – the density of the material up to the Hugoniot elasticity limit;  $G$  – the shear modulus of the material;  $k_1$  – a coefficient equivalent to the bulk modulus of elasticity;  $k_2$  and  $k_3$  – the coefficients. The relationship between the bulk modulus of elasticity and Young's modulus is determined by the equation

$$K = \frac{E}{3(1-2\nu)}. \quad (9)$$

The component of the stress at the Hugoniot elastic limit is determined by formula (6), in which the corresponding density of the material is assumed.

In a simplified form, formula (8) can be written

$$\sigma_{hel} = 1.5(\tau_{hel} - p_{hel}). \quad (10)$$

It is necessary to separately mention the parameters that are clearly not included in the dependencies described above, but require determination when modeling high-speed loads. So, in the program map there is a parameter EPS0, which determines the threshold of the deformation rate at which the material is considered to be loaded quasi-statically. That is, if the deformation rate is less than this parameter, the material behaves quasi-statically. Otherwise, when the deformation rate exceeds the parameter EPS0, the program starts to act with a logarithmic increase in strength, which is controlled by another parameter –  $s$ .

The second parameter FS, which is the criterion for removing the material. That is, when an element is considered destroyed, it can be removed from the computational grid to simulate cracks or material destruction.

Based on the above, the corresponding parameter values were taken within the permissible limits for granite. The stress pattern in the z-axis direction and the equivalent Mises stress are presented in Fig. 2.

It follows from Fig. 2 that during impact loading, maximum stresses occur on the impact surface, as well as in places near the internal supports of the beam. Based on this statement, it can be assumed that cracks can divide the beam into 3 parts. In addition to the stress pattern, the internal and kinetic energies were also determined, the graphs of which are presented in Fig. 3, 4.

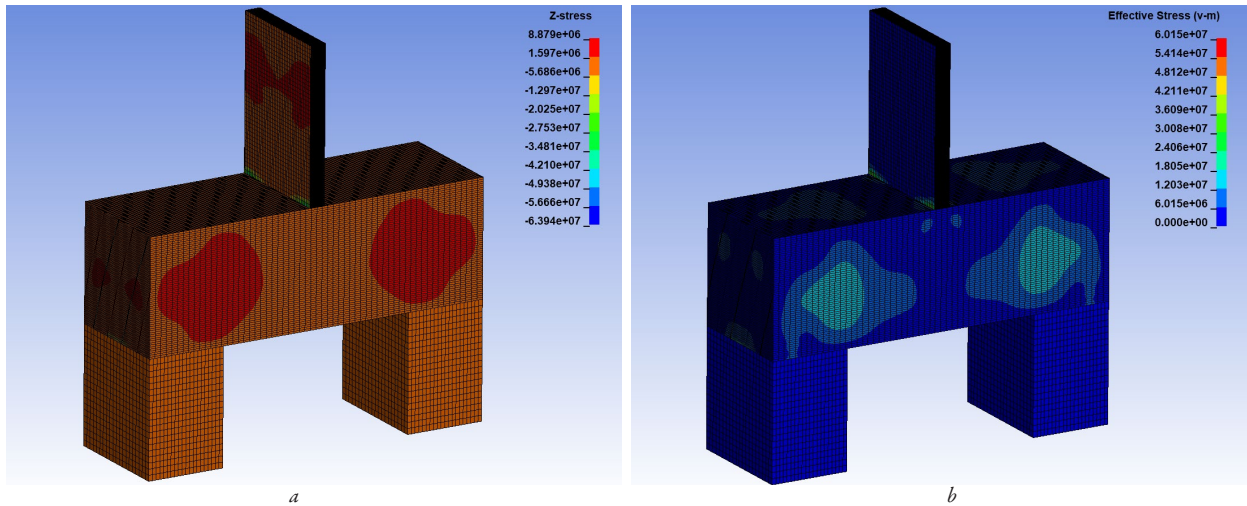


Fig. 2. Stress pattern under impact load on a beam, using the JH2 model: *a* – stress in the direction of the Z axis; *b* – equivalent Mises stresses

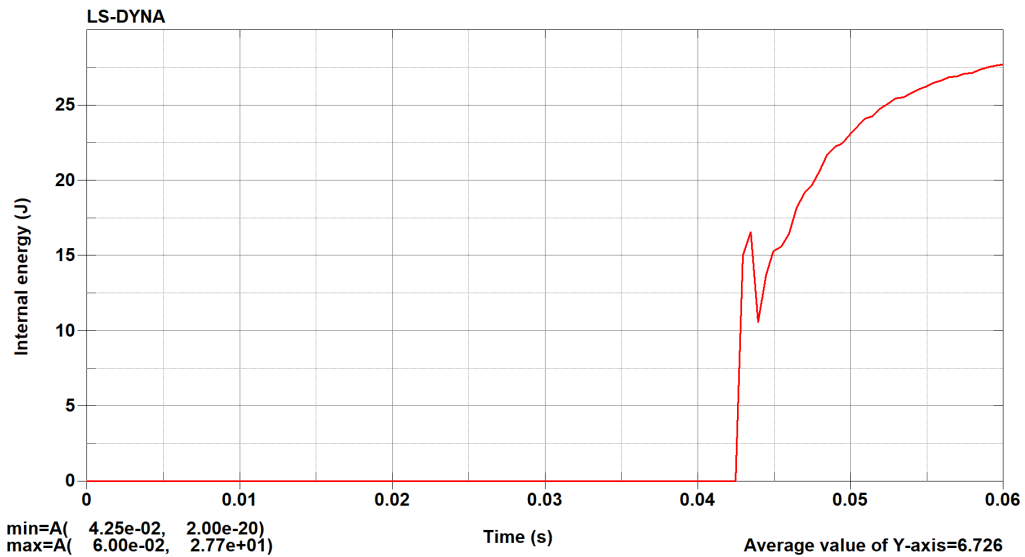


Fig. 3. Change in internal energy of the system under JH2

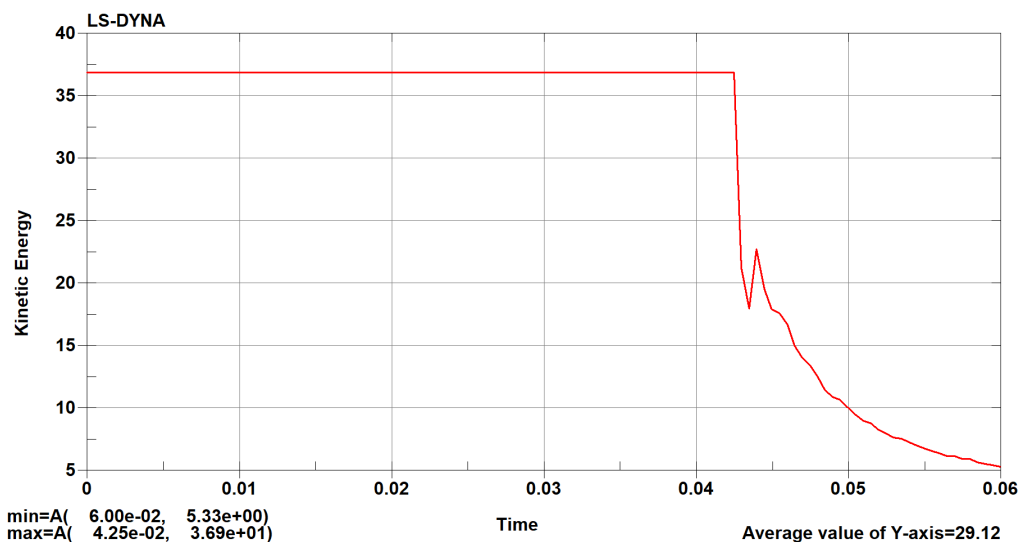


Fig. 4. Change in kinetic energy under dynamic loading of the body JH2

A comparison of energies (Fig. 3, 4) shows what part of the kinetic energy has been converted into internal energy of deformations and damage. It should be noted here that during impact, part of the kinetic

energy also goes to work on friction and damping forces at the impact site. This part of the energy is reflected by the Sliding Interface Energy program parameter, the change of which is presented in Fig. 5.

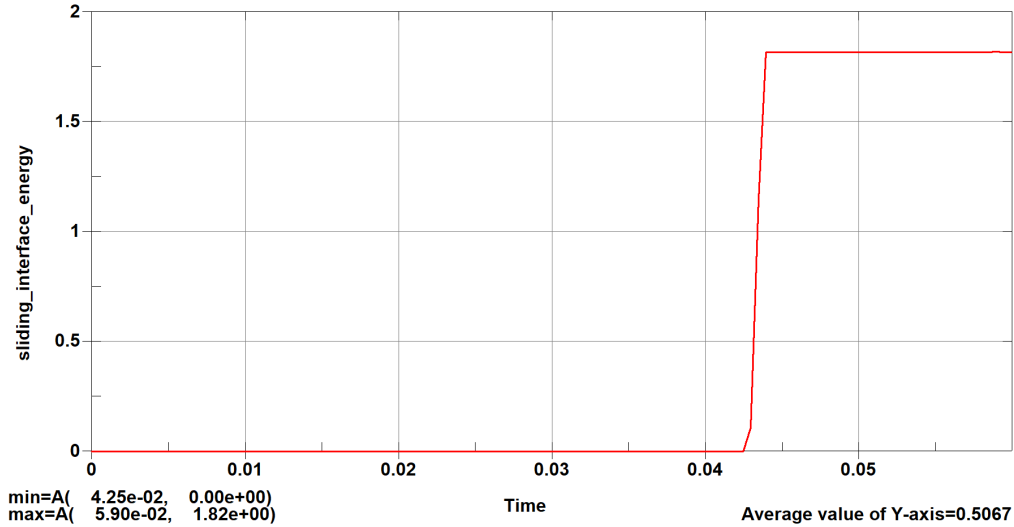


Fig. 5. Change in energy spent on contact and damping at JH2

As follows from the graph in Fig. 5, the maximum value of Sliding Interface Energy is 1.82 J.

Next, let's consider the JH1 or Mat\_Johnson\_Holmquist\_Concrete\_JH1 model. Although the model is similar to the previous one in some respects, it also has many differences. JH1, as noted earlier, is well suited for describing porous materials or concrete. The normalized equivalent stress for the model is defined as

$$\sigma^n = \frac{\sigma}{f'_c}, \quad (11)$$

where  $\sigma$  – the equivalent stress;  $f'_c$  – the quasi-static axial compressive strength.

The following dependence is used to determine the normalized equivalent stress (11) in the program

$$\sigma^n = [A(1-D) + BP^{nN}] [1 + C \ln(\dot{\epsilon}^n)], \quad (12)$$

where  $D$  – the failure parameter;  $P^n = P/f'_c$  – the normalized pressure;  $\dot{\epsilon}^n = \dot{\epsilon}/\dot{\epsilon}_0$  – the dimensionless strain rate. The model gradually accumulates damage  $D$  from equivalent plastic deformation and from plastic volumetric deformation. The dependence that determines the gradual accumulation of damage is written

$$D = \sum \frac{\Delta \epsilon_p + \Delta \theta_p}{D_1 (P^n + T^n)^{D_2}}, \quad (13)$$

where  $\Delta \epsilon_p$  – the equivalent plastic strain;  $\Delta \theta_p$  – the volumetric plastic strain;  $D_1$  and  $D_2$  – the material constants;  $T^n = T/f'_c$  – the maximum normalized hydrostatic tensile pressure.

Strength at a certain damage ( $DS$ ), provided that  $P^n > 0$  and the action of compressive loads

$$DS = f'_c \min \left[ \sigma_{\max}, A(1-D) + BP^{nN} \right] [1 + C \ln \dot{\epsilon}^n], \quad (14)$$

under the action of tensile loads and  $P^n < 0$

$$DS = f'_c \max \left[ 0, A(1-D) - A \left( \frac{P^n}{T} \right) \right] [1 + C \ln \dot{\epsilon}^n], \quad (15)$$

where  $A$  – the normalized cohesive strength;  $C$  – the strain rate coefficient;  $N$  – the exponential index of strengthening under pressure;

$\sigma_{\max}$  – the maximum allowable strength of the material in the normalized form;  $B$  – the normalized strengthening under pressure.

The pressure for a completely dense material is determined

$$P = k_1 \theta' + k_2 \theta'^2 + k_3 \theta'^3, \quad (16)$$

where  $k_1, k_2, k_3$  – the material constants;  $\theta'$  – the modified volumetric strain.

Modified volumetric strain is defined

$$\theta' = \frac{\theta - \theta_{lock}}{1 + \theta_{lock}}, \quad (17)$$

where  $\theta_{lock}$  – the closed volumetric strain.

Here it is necessary to give an explanation of the above dependencies. Closed volumetric strain is a strain at which the material becomes completely compacted, i. e. after this deformation, additional compression of the material is no longer possible. That is, here it is necessary to imagine that there may be pores in the rock, which are closed during deformation. Modified volumetric strain is a corrected strain that is used to determine the pressure and behavior of the material, taking into account that the material may not always be dense.

The stress pattern (Fig. 6) reflects the first seconds of the impact. As is seen, there are differences between these patterns. The maximum stresses are clearly expressed at the point of impact and contact of the beam with the inner faces of the beam supports.

The change in internal and kinetic energies is shown in Fig. 7, 8. The maximum value of internal energy is 21.6 J.

The change in contact interaction energy is shown in Fig. 9, the maximum value of which is 3.47 J.

### 3.2. Experimental studies of dynamic fracture of materials with different physical and mechanical properties

The results of the experimental studies were listed in Table 1.

Fig. 10, a shows the samples that were tested, the characteristic fracture on the example of sample No. 1 is shown in Fig. 10, b.

The following parameters are included in Table 1:

- 1)  $E_s$  – total fracture energy;
- 2)  $E_1$  – energy per fracture site;
- 3)  $E_{spec}$  – specific fracture energy, related to the cross-sectional area of the sample.

Based on the data (Table 1), an analysis of the distribution of the spent fracture energy depending on the cross-sectional area of the sample was performed (Fig. 11).

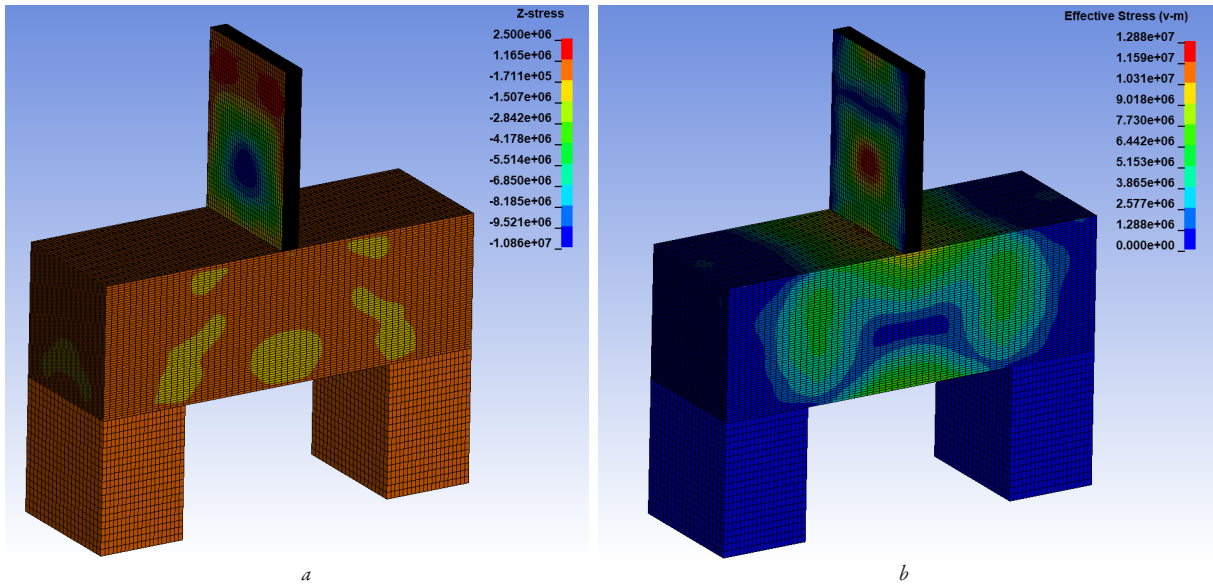


Fig. 6. Stress pattern under impact load on the beam, rheological model of beam JH1: *a* – stresses in the direction of the Z axis; *b* – equivalent Mises stresses

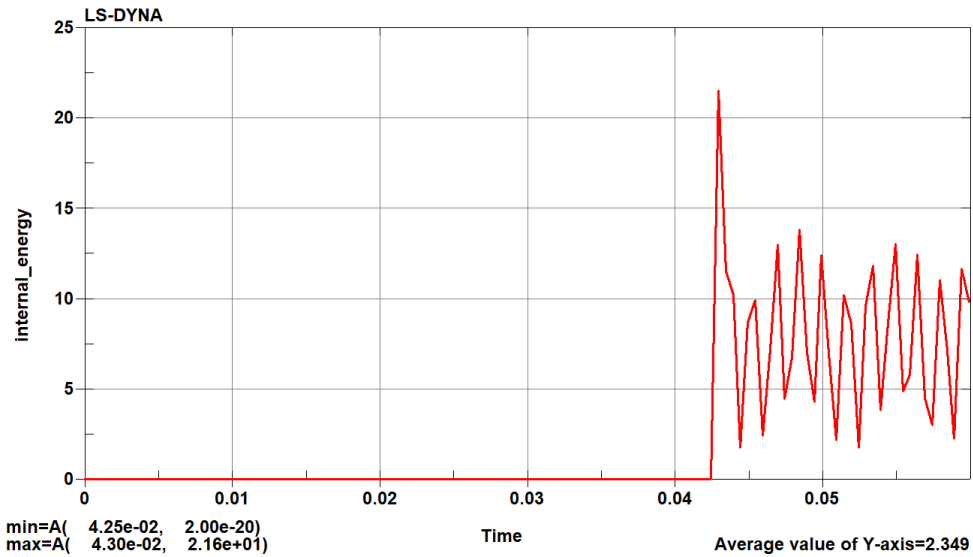


Fig. 7. Change in internal energy of the system at JH1

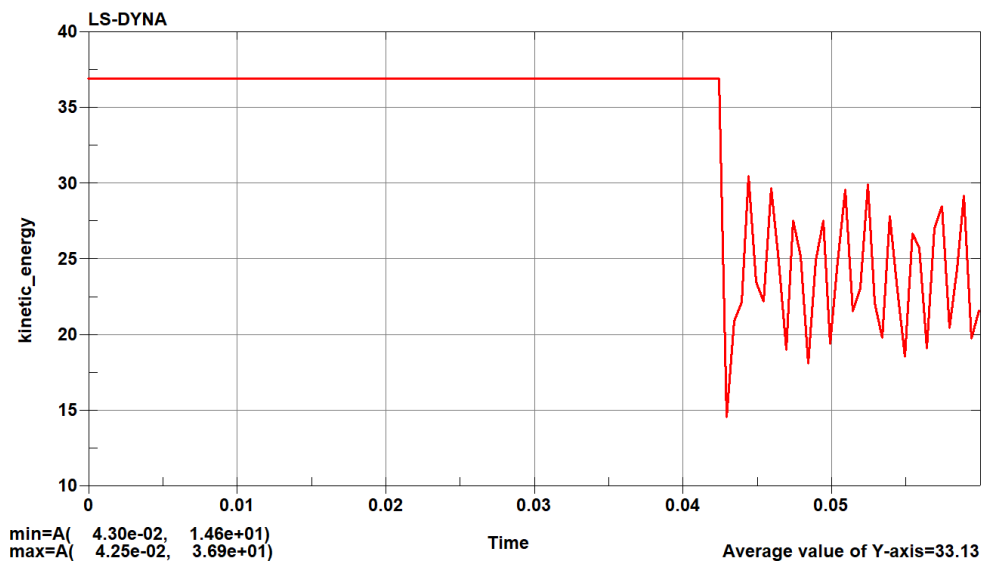


Fig. 8. Change in kinetic energy at dynamic loading of the body JH1

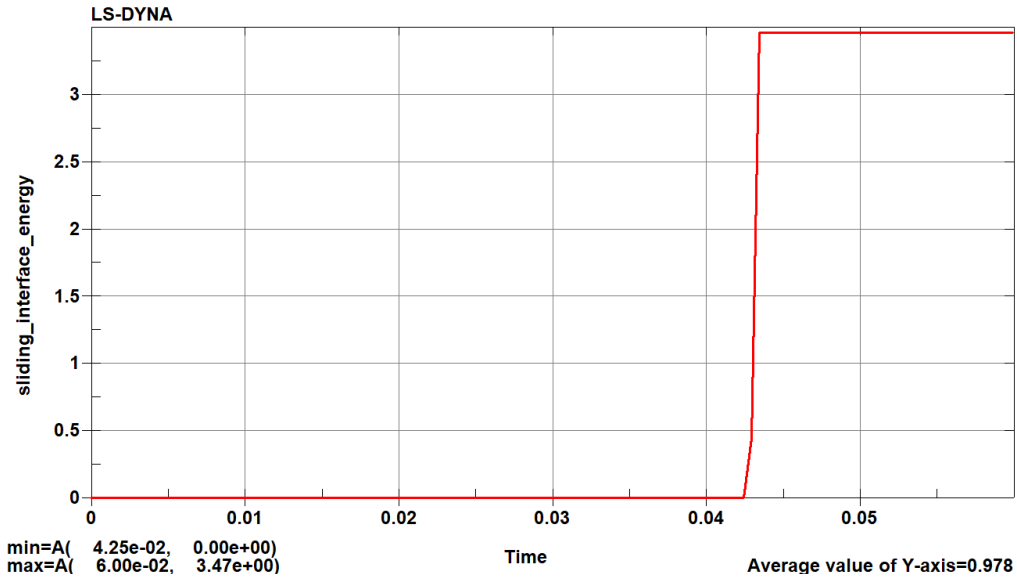


Fig. 9. Change in energy spent on contact and damping at JH1

Table 1

Results of experimental studies

Cross-section characteristics				Results obtained				
Sample No.	Cross-sectional area, m <sup>2</sup>	Length, mm	Type	$\alpha$	$\beta$	$E_s, J$	$E_1, J$	$E_{spec}, J$
1	0.00142	405	granite	33.187	15.142	27.796	13.898	9787
2	0.00142	210	granite	40.432	33.637	15.454	15.454	10883
3	0.00071	98	granite	47.79	37.26	26.854	26.854	37822
4	0.00179	65	granite	69.48	59.535	33.875	33.875	18924
5	0.00121	65	gabbro	62.325	58.41	12.855	12.855	10623
6	0.00121	60	gabbro	62.19	52.695	30.204	30.204	24962
7	0.00123	217	gabbro	47.745	40.005	20.254	10.127	8233
8	0.00247	98	marble	62.235	49.05	41.036	10.259	4153
9	0.0011	106	marble	62.46	57.015	17.763	17.763	16148
10	0.00138	108	marble	62.257	54.472	25.025	25.025	18134



Fig. 10. General view of the samples: *a* – before testing; *b* – destroyed sample No. 1

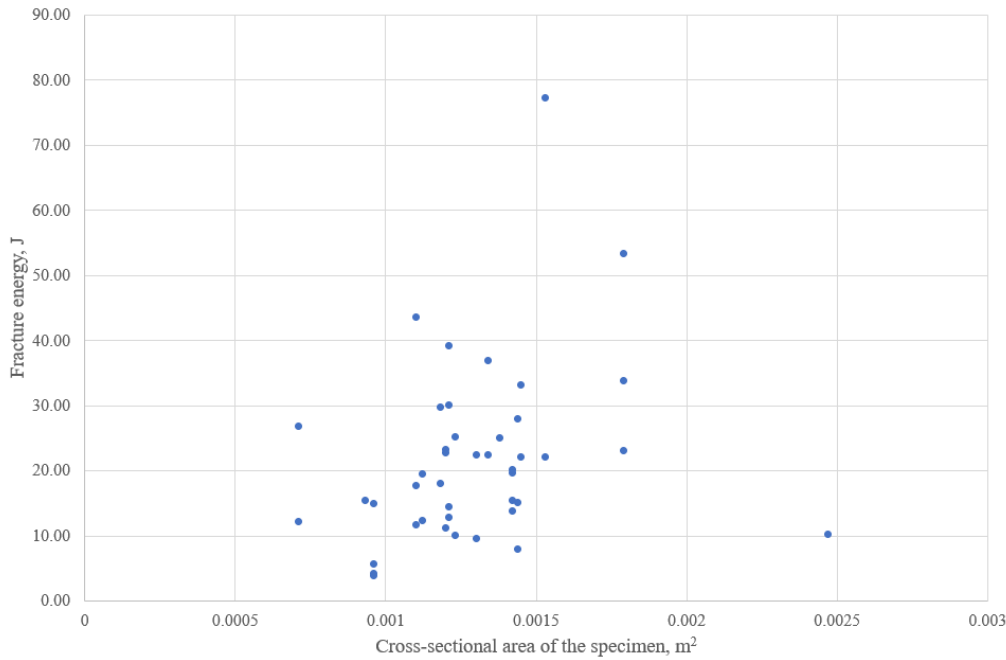


Fig. 11. Distribution of the fracture energy of the sample depending on its cross-sectional area

**3.3. Determination of the resistance coefficient for different rocks based on experimental data**

The study of the effect of velocity on the fracture parameters was carried out based on the equation of free oscillations of the pendulum

$$m\ddot{x} + b\dot{x} + cx = 0, \tag{18}$$

where  $m$  – the mass of the pendulum;  $b$  and  $c$  – the resistance coefficient (Ns/m) and the elasticity coefficient (N/m);  $x$  – displacement, m.

The general solution of equation (18) has the following form

$$x = e^{-bt/2m} (A_1 \cos(\omega_0 t) + A_2 \sin(\omega_0 t)). \tag{19}$$

Based on (19) the solution of equation (18) an expression for determining the frequency of natural oscillations is obtained

$$\omega_0 = \sqrt{\frac{c}{m} - \left(\frac{bt}{2m}\right)^2}. \tag{20}$$

The elasticity of the system is determined by the formula

$$A = \omega_0^2 m. \tag{21}$$

The indicator  $bt/2m$  in formula (20) reflects the resistance and the rate of damping of oscillations of the system and is the logarithmic decrement of oscillations

$$\delta = \ln \frac{x_n}{x_{n+1}}, \tag{22}$$

where  $x_n, x_{n+1}$  – the amplitude of the damping oscillations corresponding to the beginning and end of the oscillation period.

The logarithmic decrement of oscillations  $\delta$  can also be determined through the energy absorption coefficient  $\psi$

$$\psi = 2\delta, \tag{23}$$

where  $\psi = \Delta E/E$ ;  $\Delta E = E_s$  – the energy absorbed by the system during one oscillation period;  $E$  – the total energy of the system.

Then, taking into account the condition  $\psi = \Delta E/E$ , the dependence (23) will have the form

$$\delta = \frac{\Delta E}{2E}. \tag{24}$$

Based on (23) and (24), the formula for determining the resistance coefficient will have the form

$$b = \frac{\Delta E c}{2E \pi \omega}. \tag{25}$$

For the numerical values from the experiment  $m = 21.318$  kg for  $\omega_0 = 4.188$  and  $c = 374.045$  n/m and taking into account (25), the values of the parameters were obtained to assess the influence of speed on the fracture parameters (Table 2).

Table 2

Numerical values of the parameters

No.	$\psi$	$\delta$	$E_s, J$	$b$	$v, m/s$
1	0.843	0.421	32.951	11.996	1.757
2	0.32	0.160	48.246	4.555	2.126
3	0.405	0.202	66.292	5.761	2.492
4	0.258	0.129	131.204	3.671	3.506
5	0.118	0.059	108.19	1.689	3.184
6	0.28	0.140	107.768	3.985	3.178
7	0.306	0.153	66.175	4.352	2.49
8	0.38	0.190	107.909	5.408	3.179
9	0.204	0.102	107.768	2.914	3.178
10	0.714	0.357	108.19	10.167	3.184

Further, using the obtained results, graphs of the change in the dynamic coefficient versus relative frequency for different materials were constructed (Fig. 12).

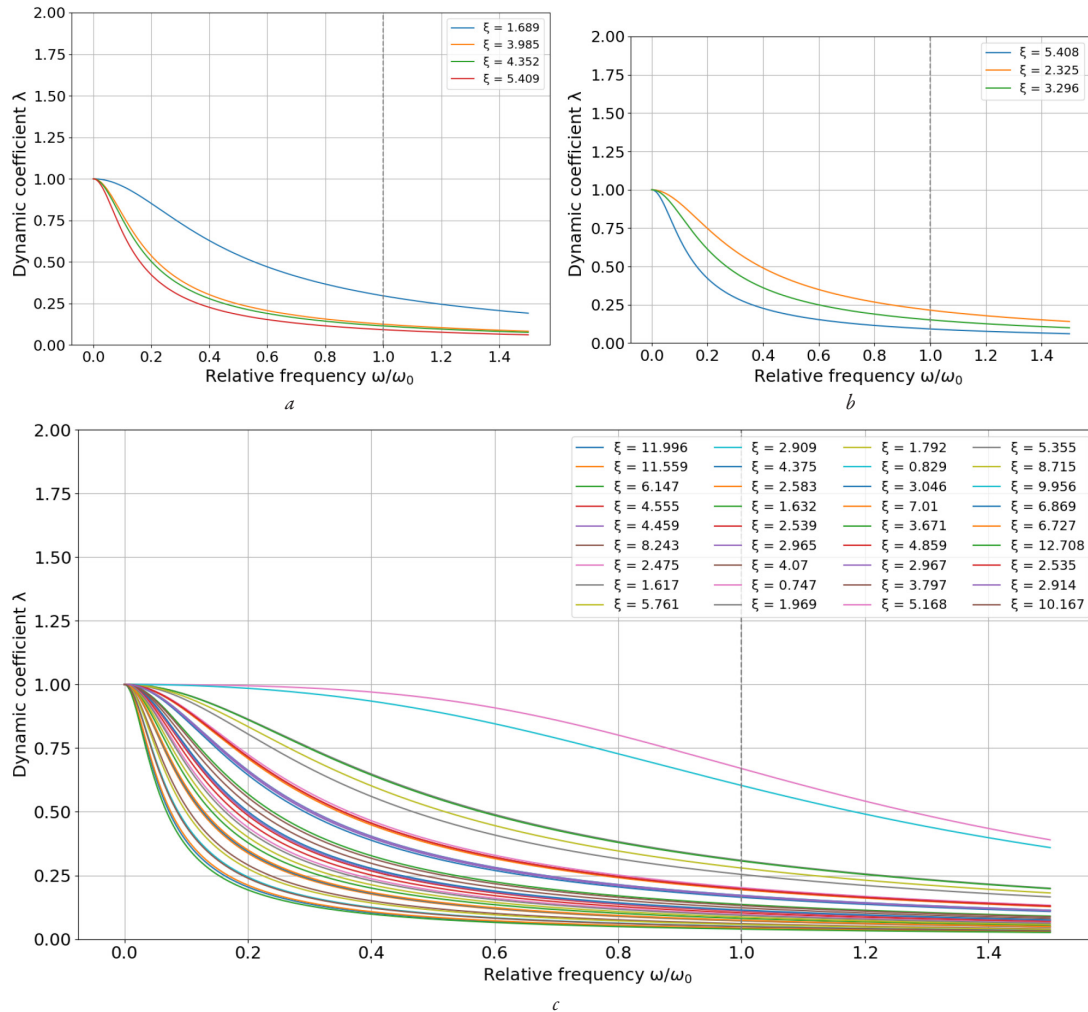


Fig. 12. Dependence of the dynamic coefficient on the relative frequency: *a* – gabbro; *b* – marble; *c* – granite

The graphs given are an estimate of the energy consumption during the destruction of materials that have different physical properties. At the same time, it was found from the obtained destructions of the samples that the crack surface, namely its cut, is different in the energy consumption for the destruction process of individual samples.

Analyzing the graphs of Fig. 3–5, which correspond to the rheological model JH2, a difference was noted in the energy supplied to the sample due to impact and the energy usefully spent on internal deformations that lead to its destruction. The difference in total is  $E_k - E_m = 36.9 - 27.7 = 9.2$  J. Thus, it can be noted that during the impact, a part of the energy in the amount of 9.2 J is dissipated and does not go to the useful work of deformation of the body. The dissipated energy includes the energy of contact interaction, which is 1.82 J.

When studying the rheological model JH2 (Fig. 7–9), it was found that the difference between the supplied energy and the energy spent on useful work reaches 15.3 J.

From the scattering of the data presented in Fig. 13, it follows that the total supplied energy of fracture of the sample with a cross-sectional area within 0.001–0.0015 m<sup>2</sup> has a value of 10–30 J. Thus, it can be noted that a significant part of the energy is spent on accompanying processes: the formation of fragments, elastic waves, microfracture in the volume, heat and friction, losses in the installation supports. And not a significant part goes to the formation of cracks.

The scatter of the data can be explained by the following statements. In the destruction of polycrystalline materials, grain boundaries play a large role and the grain size is an important structural parameter that determines the regularity of this process. In intergranular fracture,

grain boundaries are barriers to mobile dislocations and contribute to the formation of dislocation clusters. Therefore, grain boundaries are the best place for crack initiation and crack propagation.

In intragranular fracture, grain boundaries are obstacles to crack propagation. A crack can cross the boundary without changing its trajectory only in the case of very small angles of mutual orientation of crystals. In other cases, the grain boundary is an insurmountable obstacle to crack development. If a crack nevertheless crosses the intergranular boundary, then under the action of local stress concentration in the crack breakthrough zone, new cracks appear in the corresponding cleavage planes of neighboring grains. The formation of new cracks and cleavage steps when they merge – all this requires additional energy input to the sample and prevents the propagation of the main crack.

Thus, for samples with a homogeneous structure, the crack development occurs according to the intergranular mechanism, respectively, the sample is destroyed in one plane with the expenditure of minimal energy. In the case of an impact on a solid grain, the crack is initiated on both sides of the grain, as a result of which the destruction occurs in at least two planes. The result of such an action is the separation of the sample into three or more parts. Another case of the occurrence of a fracture plane that has an angle with the plane of the cross-section of the sample. In this case, the main crack falls on the boundary of grain separation, as a result of which it begins to move along the boundary, itself changing the direction of movement.

Analyzing the graph of Fig. 12, it should be noted that the range of change of the dynamic coefficient curve is somewhat wide, this is

explained by additional factors that must be taken into account. The obtained result is explained by the different origin of the tested samples, which are selected from several deposits. Also, the structure of the grains and their orientation relative to the impactor were not taken into account before the test. These factors are decisive and affect the energy required for the destruction of materials. A special case is when the load is applied to the grain boundary interface, but a solid grain is located in the path of the crack, then the crack can go around the grain surface, changing the direction of movement. All this leads to differences in the energy expended for destruction. In work [6], crack branching during dynamic destruction is studied, but the values of the crack propagation energy for different materials are not given. Instead, a scale parameter is introduced – the ratio of the fracture energy to the elastic modulus. In addition, for the quality of experimental data, polyacrylamide gel is used in the work, which may introduce a corresponding error when transferring the results to rocks. On the other hand, it is proved that the energy required to create a unit area of a crack affects its trajectory, but it is not clear how energy dissipation is taken into account. It should be noted separately that the work does not specify the rate of load application, but only the rate of crack propagation, which complicates the assessment of the correlation of the research results with real fracture processes in machines. In the source [7], the fracture energy is taken as an input parameter for the study of crack formation in concrete. To describe the behavior of the material, a nonlinear damage model based on the concept of distributed cracks is used. The damage itself in the model is determined on the basis of the stress-strain curve. The advantages of the Johnson-Holmquist model are the ability to determine a physically justified value of the accumulated damage, which allows taking into account the effect of the deformation rate. In the model used in [7], material damage is taken into account implicitly, and through the stress drop due to the achievement of peak strength. In addition, it should be noted that the work does not consider the issue of energy dissipation, but proposes a numerical model for modeling crack growth under conditions of applying dynamic loads. Similarly to the study [6], the work does not specify the speed limit for applying dynamic loads to a concrete structure.

The research results can be used in the development and study of equipment for crushing materials. The value of the specific fracture energy can be used to study dynamic processes in building structures under excessive loads.

### 3.4. Limitations and directions of research development

The research concerns materials of natural origin and cannot be used to analyze similar processes for artificial materials, which limits the application of the obtained results.

However, the used method for determining the fracture energy can be applied to building materials in the study of crushing and reuse processes, which requires additional research. An important factor is the shape of the sample surface, its initial dimensions and conditions of fixation. Determining the patterns of influence of such factors is a promising direction of this research and is planned by the authors in further projects.

A quantitative assessment of the effect of implementing the research results can be estimated on the basis of a series of further studies, since the task is complex in relation to crushing machines. But in general, it can be noted that taking into account the energy and force parameters of the material fracture process, which are accompanied by the formation of a crack, the dissipation of part of the energy into the contact interaction, and also taking into account energy losses in the machine components, the geometry of the crushing plates and the operating parameters of the power equipment can be optimized. On the other hand, the research results encourage the search and creation of energy-efficient crushing equipment, which will use the principle of directional material destruction.

## 4. Conclusions

1. The work performed numerical modeling of the destruction process of prismatic samples using the LS-DYNA software, determined the corresponding stresses and deformations and established the values of the corresponding energy costs, namely the change in kinetic energy, the energy spent on contact interaction 1.82 J. For the JH2 model, the difference between the supplied energy and the energy spent on useful work reaches 15.3 J. The Johnson Holmquist Ceramics model is better suited for describing brittle materials, while the Johnson Holmquist Concrete model is better suited for describing concrete and materials with combined behavior, where it is important to take into account, in addition to brittleness, plasticity and frictional effects (internal and interfacial friction in the material).

2. Based on experimental studies, the energy costs of the process of dynamic destruction of rocks were determined. For a sample cross-sectional area of 0.001 m<sup>2</sup> to 0.0015 m<sup>2</sup>, the total energy expended on the dynamic fracture process is within 10–30 J. This value takes into account the sum of the process energies: formation of fragments, elastic waves, microfracture in the volume, heat and friction, losses in the installation supports, and crack formation. For each sample, resistance coefficients were calculated, on the basis of which the corresponding amplitude-frequency characteristics of the dependence of the dynamic coefficient on the relative frequency for the corresponding material were constructed. Numerical modeling of the loading process of samples, taking into account experimental data and based on the Johnson Holmquist Ceramics and Johnson Holmquist Concrete models, was performed in order to reflect the stresses and strains that arise in the material under conditions when the material does not collapse. When the load application rate approaches that in the experiment, significant mesh deformations occur in the finite element model, which indicates fracture. The difference in kinetic energy between theory and experiment is 14%.

3. It is proposed to estimate the dissipated energy based on the corresponding resistance coefficient. Using experimental data, the ranges of change in the resistance coefficient values are established:

- 1) granite – 0.747–11.996;
- 2) gabbro – 1.689–5.409;
- 3) marble – 2.325–5.408.

## Conflict of interest

The authors declare that they have no conflict of interest regarding this research, including financial, personal, authorship or other, that could influence the research and its results presented in this article.

## Financing

The research was conducted without financial support.

## Data availability

The manuscript has no related data.

## Use of artificial intelligence

The authors confirm that they did not use artificial intelligence technologies when creating the presented work.

## Authors' contributions

*Ivan Nazarenko*: Project administration, Conceptualization, Methodology, Validation, Supervision, Writing – review and editing;  
*Oleg Dedov*: Conceptualization, Methodology, Validation, Investigation,

Supervision, Writing – review and editing; **Yevhen Mishchuk**: Formal analysis, Investigation, Visualization, Writing – original draft; **Iryna Berynk**: Validation, Formal analysis, Writing – original draft; **Artur Onyshchenko**: Resources, Funding acquisition; **Mykola Kuzminets**: Resources, Funding acquisition; **Valentyn Chernysh**: Writing – original draft, Visualization; **Mykola Nesterenko**: Validation, Formal analysis, Writing – original draft.

## References

1. Dedov, O., Vabishchevych, M., Skoruk, O., Twardowski, G. (2024). Study of the Effects of Natural And Man-Made Origin On the Technical Condition of Architectural Monuments. *International Journal of Conservation Science*, 15 (SI), 195–204. <https://doi.org/10.36868/ijcs.2024.si.16>
2. Casagrande, L., Villa, E., Nespoli, A., Occhiuzzi, A., Bonati, A., Auricchio, F. (2019). Innovative dampers as floor isolation systems for seismically-retrofit multi-storey critical facilities. *Engineering Structures*, 201, 109772. <https://doi.org/10.1016/j.engstruct.2019.109772>
3. Yue, Y., Wang, H., Zhang, S. (2024). Dynamical Modeling and Dynamic Characteristics Analysis of a Coaxial Dual-Rotor System. *Journal of Dynamics, Monitoring and Diagnostics*, 3 (2), 99–111. <https://doi.org/10.37965/jdmd.2024.524>
4. Mishchuk, Y., Nazarenko, I. (2023). Analysis of the energy laws of material destruction. *Strength of Materials and Theory of Structures*, 110, 294–315. <https://doi.org/10.32347/2410-2547.2023.110.294-315>
5. Kammer, D. S., McLaskey, G. C., Abercrombie, R. E., Ampuero, J.-P., Cattania, C., Cocco, M. et al. (2024). Earthquake energy dissipation in a fracture mechanics framework. *Nature Communications*, 15 (1). <https://doi.org/10.1038/s41467-024-47970-6>
6. Chen, C.-H., Bouchbinder, E., Karma, A. (2017). Instability in dynamic fracture and the failure of the classical theory of cracks. *Nature Physics*, 13 (12), 1186–1190. <https://doi.org/10.1038/nphys4237>
7. Zhou, X., Jia, Z. (2024). Dynamic propagation of moving cracks in brittle materials by field-enriched finite element method. *Engineering Fracture Mechanics*, 305, 110177. <https://doi.org/10.1016/j.engfracmech.2024.110177>
8. Kamran, M., Liu, H., Fukuda, D., Jia, P., Min, G., Chan, A. (2025). State-of-the-Art Review and Prospect of Modelling the Dynamic Fracture of Rocks Under Impact Loads and Application in Blasting. *Geosciences*, 15 (8), 314. <https://doi.org/10.3390/geosciences15080314>
9. Nazarenko, I., Dedov, O., Berynk, I., Pereginets, I., Titova, L., Rogovskii, I., Ruchynskiy, M.; Nazarenko, I. (Ed.) (2021). Research of technical systems of processes of mixing materials. *Dynamic processes in technological technical systems*. Kharkiv: TECHNOLOGY CENTER PC, 57–76. <https://doi.org/10.15587/978-617-7319-49-7.ch4>
10. Javed, R. A., Zhu, S. F., Farid, M. (2013). Dynamic Fracture Toughness: Critical Review of Materials and Developments. *Applied Mechanics and Materials*, 389, 289–297. <https://doi.org/10.4028/www.scientific.net/amm.389.289>
11. Nazarenko, I., Dedov, O., Mishchuk, Y., Slipetskyi, V., Delembovskiy, M., Zalizko, I., Nesterenko, M.; Nazarenko, I. (Ed.) (2021). Research of stress-strain state of elements of technological technical constructions. *Dynamic processes in technological technical systems*. Kharkiv: TECHNOLOGY CENTER PC, 140–179. <https://doi.org/10.15587/978-617-7319-49-7.ch8>
12. Vabishchevych, M., Dedov, O., Diachenko, O., Lytvyn, O. (2025). Research of the design of a T-shaped node of cold-rolled profiles, the connection of which is made by a plate using a bolt connection. *Strength of Materials and Theory of Structures*, 114, 62–75. <https://doi.org/10.32347/2410-2547.2025.114.62-75>
13. Li, P., Liu, Y., Zhang, J., Dong, Z., Wu, X., Miao, S., Cai, M. (2025). Dynamic Failure Mechanism and Fractal Features of Fractured Rocks Under Quasi-Triaxial Static Pressures and Repeated Impact Loading. *Fractal and Fractional*, 9 (2), 71. <https://doi.org/10.3390/fractalfract9020071>
14. Li, M., Zhu, F., Mao, Y., Pu, H., Chen, Y., Wu, P., Wu, B. (2025). Dynamic direct tensile mechanical response characteristics and damage fracture mechanism of water-saturated frozen sandstone. *Journal of Materials Research and Technology*, 35, 4955–4974. <https://doi.org/10.1016/j.jmrt.2025.02.153>
15. Titov, D., Zahorsky, D., Hryhoriev, Y., Balyk, S., Kozariz, V. (2025). Experimental specification of the nature of rock mass fragmentation by blasting of borehole charges of variable length. *Technology Audit and Production Reserves*, 3 (1 (83)), 78–85. <https://doi.org/10.15587/2706-5448.2025.331974>
16. Zhang, K., Zhang, L., Liu, F., Yu, Y., Wang, S. (2024). Quantitative investigation of rock dynamic failure using Voronoi-based discontinuous deformation analysis. *Geomechanics and Geophysics for Geo-Energy and Geo-Resources*, 10 (1). <https://doi.org/10.1007/s40948-024-00767-9>
17. Javed, R. A., Shifan, Z., Guo, C., Vecchio, K. S., Jiang, F. (2015). Investigation into dynamic response of a three-point bend specimen in a Hopkinson bar loaded fracture test using numerical methods. *Advances in Mechanical Engineering*, 7 (7). <https://doi.org/10.1177/1687814015591315>
18. Wu, Y., Yin, T., Liu, X., Tan, X., Yang, Z., Li, Q. (2022). Determination of dynamic mode I fracture toughness of rock at ambient high temperatures using notched semi-circular bend method. *Transactions of Nonferrous Metals Society of China*, 32 (9), 3036–3050. [https://doi.org/10.1016/s1003-6326\(22\)66001-1](https://doi.org/10.1016/s1003-6326(22)66001-1)

✉ **Ivan Nazarenko**, Doctor of Technical Sciences, Professor, Department of Machinery and Equipment of Technological Processes, Kyiv National University of Construction and Architecture, Kyiv, Ukraine, e-mail: nazarenko.ii@knuba.edu.ua, ORCID: <https://orcid.org/0000-0002-1888-3687>

**Oleg Dedov**, Doctor of Technical Sciences, Associate Professor, Department of Machinery and Equipment of Technological Processes, Kyiv National University of Construction and Architecture, Kyiv, Ukraine, ORCID: <https://orcid.org/0000-0001-5006-772X>

**Yevhen Mishchuk**, PhD, Associate Professor, Department of Machinery and Equipment of Technological Processes, Kyiv National University of Construction and Architecture, Kyiv, Ukraine, ORCID: <https://orcid.org/0000-0002-7850-0975>

**Iryna Berynk**, Doctor of Technical Sciences, Associate Professor, Department of Processes and Equipment of Agricultural Production Processing, National University of Life and Environmental Sciences of Ukraine, Kyiv, Ukraine, ORCID: <https://orcid.org/0000-0002-1367-3058>

**Mykola Kuzminets**, Doctor of Technical Sciences, Professor, Department of Computer, Engineering Graphics and Design, National Transport University, Kyiv, Ukraine, ORCID: <https://orcid.org/0000-0002-9636-919X>

**Mykola Nesterenko**, PhD, Associate Professor, Department of Industrial Mechanical Engineering and Mechatronics, National University "Yuri Kondratyuk Poltava Polytechnic", Poltava, Ukraine, ORCID: <https://orcid.org/0000-0002-4073-1233>

**Artur Onyshchenko**, Doctor of Technical Sciences, Professor, Department of Bridges and Tunnels and Hydrotechnical Structures, National Transport University, Kyiv, Ukraine, ORCID: <https://orcid.org/0000-0002-1040-4530>

**Valentyn Chernysh**, PhD Student, Department of Bridges and Tunnels and Hydro-technical Structures, National Transport University, Kyiv, Ukraine, ORCID: <https://orcid.org/0009-0003-1993-9106>

✉ Corresponding author